VI International Conference on Textile Composites and Inflatable Structures
STRUCTURAL MEMBRANES 2013
K.-U.Bletzinger, B. Kröplin and E. Oñate (Eds)

IMPLEMENTATION OF A SIMPLE WRINKLING MODEL INTO ARGYRIS' MEMBRANE FINITE ELEMENT

RUY M.O. PAULETTI*, DANIEL M. GUIRARDI†

*Polytechnic School of the University of São Paulo
P.O. Box 61548, 05424-970 São Paulo, Brazil
Email: pauletti@usp.br, web page: http://www.lmc.ep.usp.br/people/pauletti
†IPT - Institute for Technological Research
P.O. Box 05508-901 São Paulo, Brazil
Email: dmg@ipt.br, web page: www.ipt.br

Key words: nonlinear analysis, membrane structures, Argyris' membrane element, membrane wrinkling and slackening.

Summary. This paper presents the implementation of a simple wrinkling/slackening model into the classical Argyris membrane element, comparing the solution performance by Newton's iterations, using either the tangent stiffness matrix (numerically evaluated through a finite-difference approximation), or a secant stiffness matrix (obtained through the modification of the elasticity matrix, according to a projection technique which decompose deformations into elastic and wrinkle components).

1 INTRODUCTION

There may be cases in which wrinkles on a membrane must be represented with accuracy. In these cases, a shell-like formulation is generally required, and numerical solutions require heavy computation. In the case of architectonical membranes, however, wrinkling is to be avoided, at least on the initial configuration.

To guarantee a taut surface, shape finding processes seek configurations where the minimum membrane's principal stresses are positive everywhere. In past times, this requirement was also extended to the membrane under design loads, and the onset of wrinkling was considered as a type of structural failure. Thus, in order to avoid wrinkling, high initial stresses were usually prescribed at the initial membrane configuration. Nevertheless, in practical architectonical applications, there is not an unconditional reason for the membrane to be free of wrinkles, or even slack zones, in extreme load cases, nor it is required to know the precise pattern of wrinkling, when it occurs. What does is necessary is a method capable to determine the correct load transfer mechanisms, which are distorted if the adopted finite elements do not avoid spurious compression states. Besides, if wrinkling and slackening are allowed in some conditions, the resulting anchorage loads are reduced, because smaller initial membrane stresses are then required, and also because larger membrane displacements contribute to a more favorable load distribution.

In this paper, we present the implementation of a simple wrinkling/slackening model for the classical Argyris membrane element, already available in the SATS program[1,2], and compare the performance of the tangent stiffness matrix (consistent with the proposed wrinkling/slackening model, but numerically evaluated through a finite-difference approximation), to the performance of a secant stiffness matrix (obtained when the classical linear elasticity matrix is replaced by the modified elasticity matrix derived by Akita *et al.*[3], using a projection technique to decompose deformations into elastic and wrinkle components).

2 NONLINEAR EQUILIBRIUM. VECTOR NOTATION

Upon discretization, the problem of *equilibrium of a membrane structure* can be expressed as *finding a displacement vector* $\mathbf{u}^*$ such that

$$\mathbf{g}\left(\mathbf{u}^*\right)=\mathbf{p}\left(\mathbf{u}^*\right)-\mathbf{f}\left(\mathbf{u}^*\right)=\mathbf{0} \tag{1}$$

where $\mathbf{u}=\mathbf{x}-\mathbf{x}_r$ is the *global displacement vector* with respect to a reference configuration $\mathbf{x}_r$, $\mathbf{g}\left(\mathbf{u}\right)$ is *a residual force vector*, $\mathbf{p}\left(\mathbf{u}\right)$ is the internal load vector and $\mathbf{f}\left(\mathbf{u}\right)$ is the external load vector, all of order n_{dof}, the number of degrees of freedom of the system.

These functions can be computed in sub-domains Ω^e, or elements (Figure 1(a)), as a function of the *element displacement vectors* $\mathbf{u}^e=\left[\mathbf{u}_\alpha^e\right]$, $\alpha=1,\ldots,n_n^e$, $e=1,\ldots,n^e$, where n^e is the number of elements and n_n^e is the number of nodes defining the e^{th} element. Defined onto every element, there exist an *element residual force vector* $\mathbf{g}^e=\left[\mathbf{g}_\alpha^e\right]$, where $\mathbf{g}_\alpha^e=\mathbf{g}_\alpha^e\left(\mathbf{u}^e\right)$ is the contribution of the e^{th} element to the residual vector, evaluated at its α^{th} node.

The equilibrium problem (1) can be solved –within a vicinity of a solution $\mathbf{u}^*$– iterating Newton's recurrence formula,

$$\mathbf{u}_{k+1}=\mathbf{u}_k-\left(\left.\frac{\partial\mathbf{g}}{\partial\mathbf{u}}\right|_{\mathbf{u}_k}\right)^{-1}\mathbf{g}\left(\mathbf{u}_k\right)=\mathbf{u}_k-\left(\mathbf{K}_k\right)^{-1}\mathbf{g}\left(\mathbf{u}_k\right) \tag{2}$$

where we define the *tangent stiffness matrix*

$$\mathbf{K}=\frac{\partial\mathbf{g}}{\partial\mathbf{u}}=\left[\frac{\partial g_i}{\partial u_j}\right],\quad i,j=1,\ldots,n_{dof} \tag{3}$$

Recurrence (2) may converge to a solution even when the consistent linearization of (1) is replaced by some approximation (i.e., a *secant stiffness matrix*), usually at the price of reduced convergence rate.

The element displacement vectors $\mathbf{u}^e$ can be extracted from the global one according to $\mathbf{u}^e = \mathbf{A}^e\mathbf{u}$, where $\mathbf{A}^e$ is a Boolean *incidence matrix* for that element. Likewise, the global residual force vector and the global tangent stiffness matrix can be assembled according to

$$\mathbf{g} = \sum_{e=1}^{n^e} \mathbf{A}^{eT}\mathbf{g}^e \quad \text{and} \quad \mathbf{k}^e = \frac{\partial \mathbf{g}^e}{\partial \mathbf{u}^e} = \left[\frac{\partial g_i^e}{\partial u_j^e}\right], \quad i,j = 1,\ldots,n_{dof}^e \qquad (4),\ (5)$$

where n_{dof}^e denotes the number of degrees of freedom of the e^{th} element.

3 INTERNAL LOAD VECTOR FOR A MEMBRANE ELEMENT

Figure 1 shows the Argyris' natural triangular membrane finite element, defined in an *initial configuration* Ω^0, in which it is already under an initial stress field. A *reference configuration* Ω^r usually considers stress-free conditions. For small strains, we assume $\Omega^r \equiv \Omega^0$. The element's *current configuration* is denoted by Ω^c. Element nodes and edges are numbered anticlockwise, with edges facing nodes of same number. Nodal coordinates are referred to a global Cartesian system, and a local coordinate system, indicated by an upper hat, is adapted to every element configuration, such that the $\hat{x}$ axis is always aligned with edge 3, oriented from node *1* to node *2*, whilst the $\hat{z}$ axis is normal to the element plane.

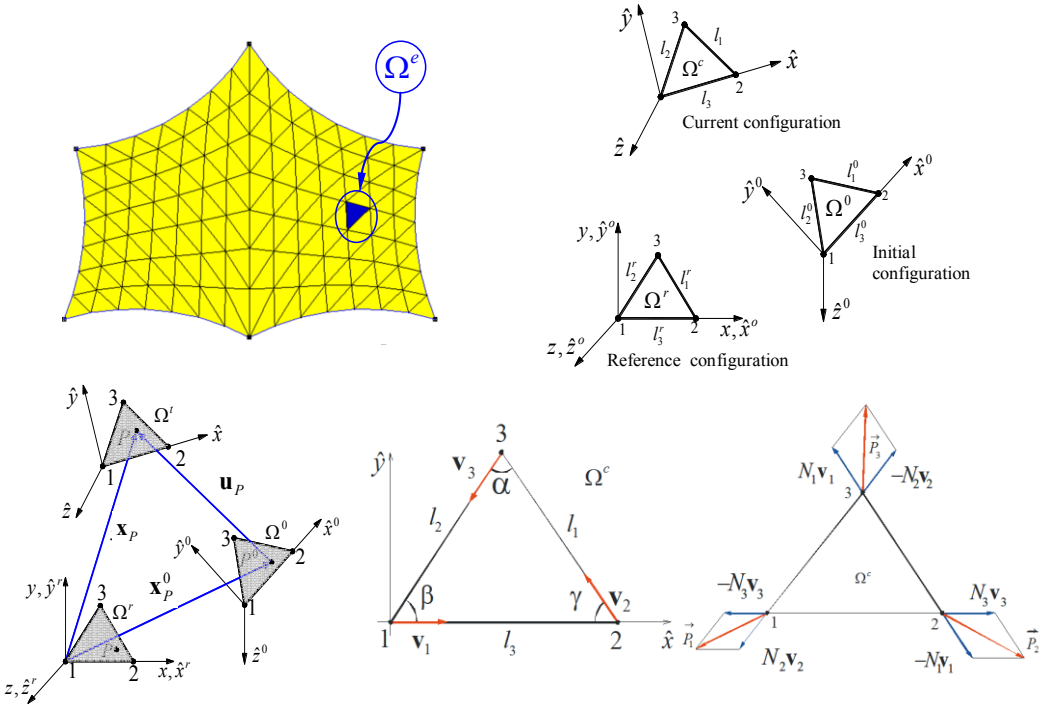

Fig. 1: (a) a domain Ω, discretized into elements Ω^e; (b) a triangular element in three different configurations; (c) position vector $\mathbf{x}_P$ and displacement vector $\mathbf{u}_P$; (d) internal angles α, β, γ and unit vectors $\mathbf{v}_i$ along the edges; (e) internal nodal forces $\mathbf{p}_i$ decomposed into natural forces $N_i\ \mathbf{v}_i$.

Fig. 1(c) displays the current global coordinates of $P \in \Omega^e$. Nodal coordinates are given by $\mathbf{x}_i = \mathbf{x}_i^0 + \mathbf{u}_i$, $i = 1,2,3$, where $\mathbf{u}_i$ are the element's nodal displacements. Fig. 1(d) displays the lengths of element edges, given by $\ell_i = \|\mathbf{l}_i\| = \|\mathbf{x}_k - \mathbf{x}_j\|$, with indexes $i, j, k = 1,2,3$ in cyclic permutation. Unit vectors parallel to the element edges are denoted by $\mathbf{v}_i = \mathbf{l}_i / \|\mathbf{l}_i\|$. With these definitions, the *vector of internal nodal forces* can be decomposed into forces parallel to the element edges, according to

$$\mathbf{p}^e = \begin{bmatrix} \mathbf{p}_1 \\ \mathbf{p}_2 \\ \mathbf{p}_3 \end{bmatrix} = \begin{bmatrix} N_2\mathbf{v}_2 - N_3\mathbf{v}_3 \\ N_3\mathbf{v}_3 - N_1\mathbf{v}_1 \\ N_1\mathbf{v}_1 - N_2\mathbf{v}_2 \end{bmatrix} = \begin{bmatrix} \mathbf{0} & \mathbf{v}_2 & -\mathbf{v}_3 \\ -\mathbf{v}_1 & \mathbf{0} & \mathbf{v}_3 \\ \mathbf{v}_1 & -\mathbf{v}_2 & \mathbf{0} \end{bmatrix} \begin{bmatrix} N_1 \\ N_2 \\ N_3 \end{bmatrix} = \mathbf{C}\mathbf{N} \qquad (6)$$

where $\mathbf{C}$ is a *geometric operator*, which collects the unit vectors parallel to the element edges and $\mathbf{N} = \begin{bmatrix} N_1 & N_2 & N_3 \end{bmatrix}^T$ is the *vector of natural forces* (see Fig. 1(d)).

We assume that the *taut behavior* of the element is linear-elastic, thus a linear relationship exists, such that

$$\mathbf{N} = \mathbf{k}_n^r \mathbf{a} + \mathbf{N}_0 , \qquad (7)$$

where $\mathbf{a} = \begin{bmatrix} \Delta\ell_1 & \Delta\ell_2 & \Delta\ell_3 \end{bmatrix}^T$, is the *vector of natural displacements* (with $\Delta\ell_i = \ell_i - \ell_i^0$, $i = 1,2,3$) and the *element natural stiffness* is a constant matrix given by

$$\mathbf{k}_n^r = V_r \boldsymbol{\mathcal{L}}_r^{-1} \mathbf{T}_r^{-T} \hat{\mathbf{D}} \mathbf{T}_r^{-1} \boldsymbol{\mathcal{L}}_r^{-1} , \qquad (8)$$

where V_r is the element volume, $\boldsymbol{\mathcal{L}}_r = \operatorname{diag}\left\{\ell_i^r\right\}$, $\hat{\mathbf{D}}$ collects the coefficients of Hooke's law for plane stresses, such that $\hat{\boldsymbol{\sigma}} = \hat{\mathbf{D}}\hat{\boldsymbol{\varepsilon}}$ and, finally, $\mathbf{T}_r$ is a transformation matrix, relating the linear Green strains $\hat{\boldsymbol{\varepsilon}}$ to the *natural strains , i.e.*, $\boldsymbol{\varepsilon}_n = \mathbf{T}_r \hat{\boldsymbol{\varepsilon}}$, highlighting the fact that Argyris' natural membrane element is akin to a *strain gauge rosette*. Explicitly we have

$$\mathbf{T}_r = \begin{bmatrix} \cos^2\gamma_r & \sin^2\gamma_r & -\sin\gamma_r\cos\gamma_r \\ \cos^2\beta_r & \sin^2\beta_r & \sin\beta_r\cos\beta_r \\ 1 & 0 & 0 \end{bmatrix} , \qquad (9)$$

where the internal angles β_r and γ_r are depicted in Figure 1(d). The upper or lower index '*r*' indicates that computations are performed in the *reference configuration*, which, for small strains kinematics, can be superimposed to the initial one. A more detailed deduction of $\mathbf{k}_n^r$ is provided in references[1,2]. Since $\mathbf{k}_n^r$ has only six independent components, its storage is usually economic, reducing the number of operations required to calculate the internal loads and tangent stiffness, and thus the overall computing time.

Inserting (7) into (6), the vector of internal forces at each configuration is given by

$$\mathbf{p}^e = \mathbf{C}\left(\mathbf{k}_n^r \mathbf{a} + \mathbf{N}_0\right). \qquad (10)$$

It is interesting to define also an *external wind load vector*, according to

$$\mathbf{f}_w^e = -\frac{pA}{3}\begin{bmatrix}\mathbf{I}_3 & \mathbf{I}_3 & \mathbf{I}_3\end{bmatrix}^T \mathbf{n}^e, \tag{11}$$

where p is a normal wind pressure acting on the element, A is its area and $\mathbf{n}^e$ its normal unit vector, in the current configuration. Thus, the *element error vector* becomes

$$\mathbf{g}^e = \mathbf{p}^e - \mathbf{f}_w^e \tag{12}$$

Proceeding with derivation of (5), the consistent *tangent stiffness matrix* of the membrane element is obtained:

$$\mathbf{k}^e = \mathbf{C}\mathbf{k}_n^r\mathbf{C}^T + \begin{bmatrix} \left(\frac{N_2}{\ell_2}\mathbf{M}_2 + \frac{N_3}{\ell_3}\mathbf{M}_3\right) & -\frac{N_3}{\ell_3}\mathbf{M}_3 & -\frac{N_2}{\ell_2}\mathbf{M}_2 \\ -\frac{N_3}{\ell_3}\mathbf{M}_3 & \left(\frac{N_1}{\ell 1}\mathbf{M}_1 + \frac{N_3}{\ell_3}\mathbf{M}_3\right) & -\frac{N_1}{\ell 1}\mathbf{M}_1 \\ -\frac{N_2}{\ell_2}\mathbf{M}_2 & -\frac{N_1}{\ell 1}\mathbf{M}_1 & \left(\frac{N_1}{\ell 1}\mathbf{M}_1 + \frac{N_2}{\ell_2}\mathbf{M}_2\right) \end{bmatrix} + \frac{p}{6}\begin{bmatrix} \mathbf{\Lambda}_1 & \mathbf{\Lambda}_2 & \mathbf{\Lambda}_3 \\ \mathbf{\Lambda}_1 & \mathbf{\Lambda}_2 & \mathbf{\Lambda}_3 \\ \mathbf{\Lambda}_1 & \mathbf{\Lambda}_2 & \mathbf{\Lambda}_3 \end{bmatrix} \tag{13}$$

$$\mathbf{k}^e = \mathbf{k}_c + \mathbf{k}_g + \mathbf{k}_{ext},$$

where $\mathbf{M}_i = \mathbf{I}_3 - \mathbf{v}_i\mathbf{v}_i^T$, $i = 1,2,3$, and $\mathbf{\Lambda}_i = \text{skew}(\mathbf{l}_i)$ are skew-symmetric matrices, whose axial vectors are given by $\mathbf{l}_i = \ell_i\mathbf{v}_i$, and where each component define, respectively, the *constitutive*, the *geometric* and the *external* components of the element tangent stiffness matrix. The contributions of $\mathbf{g}^e$ and $\mathbf{k}^e$ to (4) and (5) are given according to $\mathbf{A}_{1i}^e = \mathbf{A}_{2j}^e = \mathbf{A}_{3k}^e = \mathbf{I}_3$ and $\mathbf{A}_{1m}^e = \mathbf{A}_{2m}^e = \mathbf{A}_{3m}^e = \mathbf{O}$, $m \in \{1,2,\ldots,n_n\} \setminus \{i,j,k\}$.

4 A SIMPLE WRINKLING MODEL

Matrix $\mathbf{k}_n^r$ is constant, and provides a fast way to compute the element's internal loads and tangent stiffness, when the membrane is fully under tension, avoiding explicitly calculation of strains or stresses during solution, as they can be post-processed after equilibrium is achieved.

However, before developing compressive stresses, membranes become wrinkled or slack. Criteria for identification of the ***status*** of a membrane element (***taut*, *wrinkled* or *slack***) require consideration of stresses, strains, or both. Therefore, when wrinkling or slackening are possible, equations (10) and (13) have to be replaced for lengthier calculations. For isotropic materials, the principal stress and strain directions are parallel, and stress, strain or mixed wrinkling criteria are equivalent [7]. We choose a *pure stress criterion* and calculate element stresses directly from natural displacements.

In order to further speed up calculations, we first decompose the element natural stiffness $\mathbf{k}_n^r$ according to

$$\mathbf{k}_n^r = \left(V_r\mathcal{L}_r^{-1}\mathbf{T}_r^{-T}\right)\left(\hat{\mathbf{D}}\mathbf{T}_r^{-1}\mathcal{L}_r^{-1}\right) = \mathbf{k}_\sigma^r\mathbf{k}_a^r, \tag{14}$$

where we observe that $\mathbf{k}_{\sigma}^{r}$ and $\mathbf{k}_{a}^{r} = V_{r}^{-1}\hat{\mathbf{D}}\left(\mathbf{k}_{\sigma}^{r}\right)^{T}$ are two symmetric constant matrices that can be conveniently stored during the pre-processing phase. Then stresses in any configuration can be evaluated according to

$$\hat{\boldsymbol{\sigma}} = \mathbf{k}_{a}^{r}\mathbf{a} + \hat{\boldsymbol{\sigma}}_{0}, \qquad (15)$$

and, after calculating the principal stresses $\sigma_{1,2}$ and the "principal angle" θ_1 (between axis $\hat{x}$ and the σ_1 direction), we determine the element status and eventually modify stresses according to the following ***criterion***:

$$\begin{cases} \sigma_2 > 0 & \Rightarrow \text{TAUT} & \Rightarrow & \tilde{\hat{\boldsymbol{\sigma}}} = \hat{\boldsymbol{\sigma}} \\ \sigma_1 > 0 \wedge \sigma_2 \le 0 & \Rightarrow \text{WRINKLED} & \Rightarrow & \tilde{\hat{\boldsymbol{\sigma}}} = \dfrac{\sigma_1}{2}\left[\left(1+\cos\theta_1\right) \quad \left(1-\cos\theta_1\right) \quad \sin\left(2\theta_1\right)\right]^{T} \\ \sigma_1 \le 0 & \Rightarrow \text{SLACK} & \Rightarrow & \tilde{\hat{\boldsymbol{\sigma}}} = \mathbf{0} \end{cases} \qquad (16)$$

Thereafter, we replace (10) by (17):

$$\tilde{\mathbf{p}}^{e} = \mathbf{C}\mathbf{k}_{\sigma}^{r}\tilde{\hat{\boldsymbol{\sigma}}}. \qquad (17)$$

A mixed stress-strain criterion could avoid the intermediate calculation of negative stresses, which have no physical meaning for membranes, but by using equations (15) and (17) we determine stresses and internal loads without explicit calculation of strains, thus a stress criterion becomes more effective in our framework.

5 A FINITE-DIFFERENCE ESTIMATIVE OF THE CONSISTENT STIFFNESS MATRIX

Equation (17), inserted into (12) is all what is needed to solve the equilibrium problem through dynamic relaxation, as done for instance in reference[4]. In order to use Newton's iterations, however, also the system's tangent stiffness matrix is required. Nevertheless, instead of performing the consistent linearization of (17), we opt to evaluate it numerically, through the *finite-difference approximation* developed in references[5,6], which was shown to yield the same convergence rate and precision as the consistent tangent stiffness matrix, for highly nonlinear problems of cables, membrane and shell structures, with fairly acceptable extra computational cost. Such type of finite-difference procedures is commonly used in nonlinear mechanics, to compute approximate consistent tangent moduli, for complicated material laws $\boldsymbol{\sigma} = \boldsymbol{\sigma}\left(\boldsymbol{\varepsilon}\right)$. In our approach, however, instead of approximating the tangent modulus, we directly approximate the tangent stiffness matrix, including all nonlinear effects that might affect the global error vector $\mathbf{g}$.

First, we first partition the element tangent stiffness matrix (13) according to

$$\mathbf{k}^{e} = \left[\begin{array}{cccc} \mathbf{k}_{1}^{e} & \mathbf{k}_{2}^{e} & \cdots & \mathbf{k}_{n_{dof}^{e}}^{e} \end{array}\right] \qquad (18)$$

where column $\mathbf{k}_j = \dfrac{\partial \mathbf{g}}{\partial x_j}$ can be interpreted as the *directional derivative* of $\mathbf{g}$ with respect to the j^{th} component of $\mathbf{x}$. Thereafter, we approximate these n^e_{dof} directional derivatives $\mathbf{k}^e_j$ by a *central-difference* scheme, according to

$$\breve{\mathbf{k}}^e_j = \frac{1}{2h}\left[\mathbf{g}^e\left(\mathbf{x}^e + h\boldsymbol{\delta}^e_j\right) - \mathbf{g}\left(\mathbf{x}^e - h\boldsymbol{\delta}^e_j\right)\right],\ j = 1,\ldots,n^e_{dof}\ , \tag{19}$$

where h is a finite scalar parameter and $\pm h\boldsymbol{\delta}^e_j$ are backward and forward perturbations of the j^{th} element degree of freedom, such that $\boldsymbol{\delta}^e_j = \left[\ \delta_{ij}\ \right]$, $i = 1,\ldots,n^e_{dof}$, and where δ_{ij} is the *Kronecker delta*. Finally, inserting approximations (19) into (18), we obtain numerical estimates for the tangent stiffness matrices $\breve{\mathbf{k}}^e$, which are then assembled into a global a stiffness matrix $\breve{\mathbf{K}}$. In references[5,6] we have shown that this method provides excellent approximations for the consistent tangent stiffness matrix, as long as h is small enough. Moreover, since no extra cost is associated to reducing the size of h, it can be taken as a function of the machine precision ε, as small as possible, but without introducing numerical noise. In MATLAB environment, where SATS was implemented, we found that $h = \sqrt[4]{\varepsilon}$ is a good compromise estimative.

6 A SECANT STIFFNESS MATRIX

We have also investigated the use of a secant approximation to the stiffness matrix, by which instead of performing the consistent linearization of equation (17), we simply modify the elements' natural stiffness, equation (14), according to a modified elasticity matrix, borrowed from the paper by Akita *et al.*[3]. After decomposing the total strains on a membrane element into *elastic* and *wrinkled fractions*, according to $\hat{\boldsymbol{\varepsilon}} = \hat{\boldsymbol{\varepsilon}}_e + \hat{\boldsymbol{\varepsilon}}_w$, these authors finally arrive to

$$\hat{\boldsymbol{\varepsilon}}_w = \frac{\mathbf{s}_2\mathbf{s}_2^T\hat{\mathbf{D}}}{\mathbf{s}_2^T\hat{\mathbf{D}}\mathbf{s}_2} = \mathbf{Q}\hat{\boldsymbol{\varepsilon}}\,, \tag{20}$$

where $\mathbf{Q}$ is *a projection matrix*, that extracts the wrinkled portion of the deformation from the total one. Vectors $\mathbf{s}_1$ and $\mathbf{s}_2$ are such that $\boldsymbol{\varepsilon} = \varepsilon_1 \cdot \mathbf{s}_1 + \varepsilon_2 \cdot \mathbf{s}_2$, with ε_1 and ε_2 being the element's principal strains (never actually calculated, in our method). Explicitly,

$$\begin{cases} \mathbf{s}_1 = \dfrac{1}{2}\left[\left(1+\cos 2\theta_1\right) \quad \left(1-\cos 2\theta_1\right) \quad 2\sin 2\theta_1\right]^T \\ \mathbf{s}_2 = \dfrac{1}{2}\left[\left(1-\cos 2\theta_1\right) \quad \left(1+\cos 2\theta_1\right) \quad -2\sin 2\theta_1\right]^T \end{cases} \tag{21}$$

Now since $\hat{\boldsymbol{\varepsilon}}_w$ does not rise stresses, $\tilde{\hat{\boldsymbol{\sigma}}} = \hat{\mathbf{D}}\hat{\boldsymbol{\varepsilon}}_e = \hat{\mathbf{D}}\left(\boldsymbol{\varepsilon} - \boldsymbol{\varepsilon}_w\right) = \hat{\mathbf{D}}\left(\mathbf{I} - \mathbf{Q}\right)\boldsymbol{\varepsilon} = \tilde{\hat{\mathbf{D}}}\hat{\boldsymbol{\varepsilon}}$, where

$$\tilde{\hat{\mathbf{D}}} = \left(\mathbf{I} - \mathbf{Q}\right)\hat{\mathbf{D}} \tag{22}$$

is the *modified elasticity matrix* we seek. Inserting (22) into (14) and that into (13), we finally obtain a modified, *secant stiffness matrix*

$$\tilde{\mathbf{k}}^e = \tilde{\mathbf{k}}_c + \mathbf{k}_g + \mathbf{k}_{ext} \ , \tag{23}$$

in which only the constitutive part $\tilde{\mathbf{k}}_c$ is approximate. In principle, this non-consistent stiffness matrix may slow down convergence rates, but its use in reference[7] allowed easy solution, as shown in the following benchmark.

7 A FIRST BENCHMARK – THE 'MEMORIAL DOS POVOS'

In references[4,7] we presented results obtained by the SATS program[2] for the membrane roof of the "Memorial dos Povos de Belém do Pará", shown Figure 2, under a uniform upward wind load acting over the whole membrane surface, considering both fully-adherent and frictionless sliding border cables. A discretization much coarser than the one used in actual design was adopted, to ease the visualization of results. In the present paper, we consider only results obtained for the fully-adherent model, which can be compared also with results given by the Ansys FEM code (a sliding cable is not directly available in Ansys, thus the sliding condition was not analyzed by that program).

Figure 2: The membrane roof of the "Memorial dos Povos de Belém do Pará"

Table 1: Comparison of some selected results, for $\left(\|\mathbf{g}\| / \|\mathbf{g}_0\|\right) \le 10^{-5}$

Program	**SATS**			**Ansys**
Method	Newton (tangent $\breve{\mathbf{K}}$)	Newton (secant $\tilde{\mathbf{K}}$)	Dynamic Relaxation	Newton + line-search
Maximum displacement [m]	0.40403	0.40403	0.40343	0.40285
Maximum σ_1 [MPa]	13.60979	13.60974	13.59338	13.6
Minimum σ_1 [MPa]	5.47444	5.47442	5.47499	5.47
Maximum σ_2 [MPa]	5.37598	5.37598	5.37532	5.37
Minimum σ_2 [MPa]	0.00000	0.00000	0.00000	0.00014
Number of iterations	5	7	--	12
Time to solution [s]	4.586	4.353	--	1.747
Time per iteration [s]	0.9172	0.6218	--	0.1456

We also compare results obtained by SATS, through Newton's iterations, using both the tangent or the secant stiffness matrices ($\breve{\mathbf{k}}^e$ or $\tilde{\mathbf{k}}^e$), with those obtained through dynamic relaxation[4], a method which only requires the definition of the modified error vector $\tilde{\mathbf{g}}$, yielding an independent checking for results, besides Ansys model.

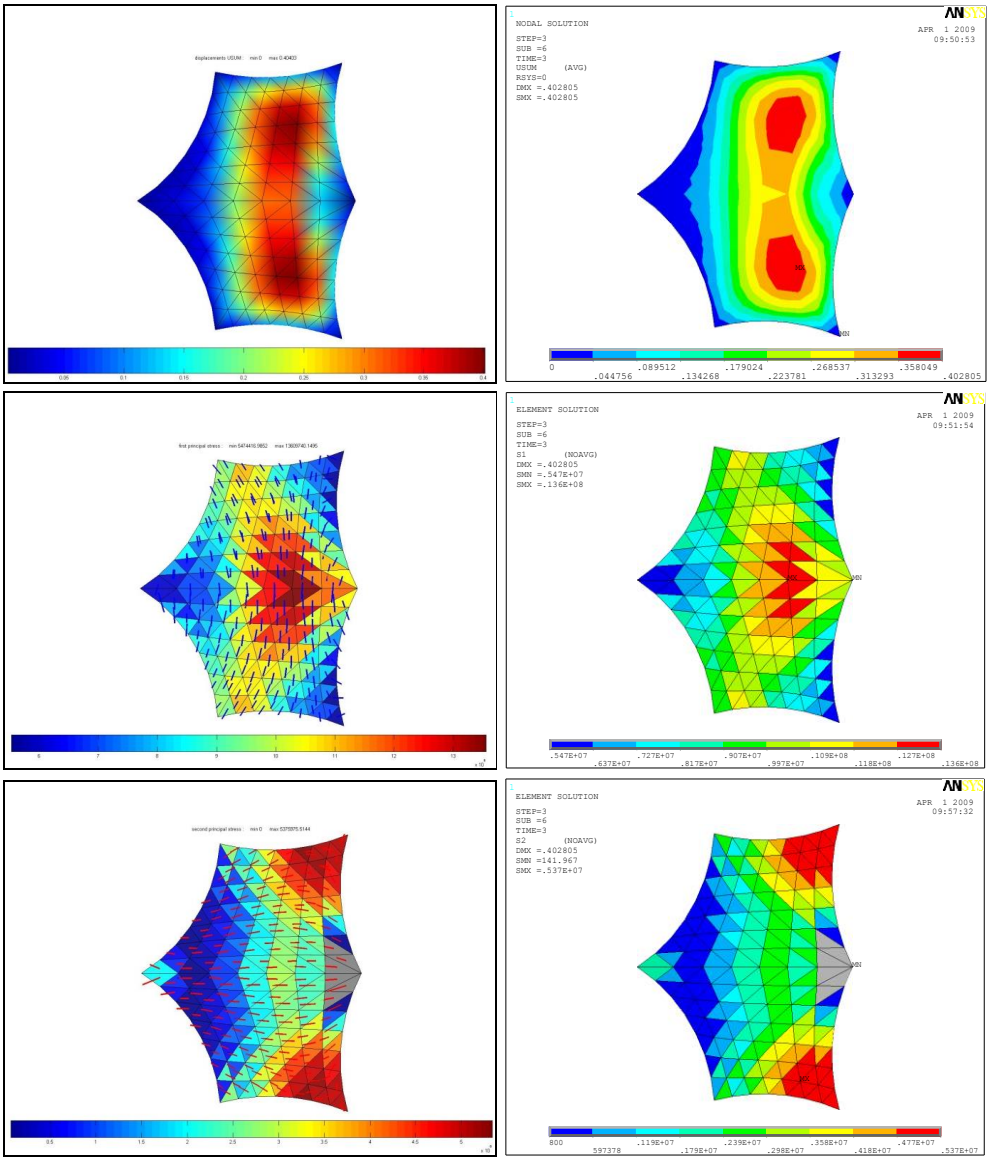

Figure 3: Results by SATS (both Newton's iterations dynamic relaxation) compared to results by Ansys; Top to bottom: displacement norms; σ_1 on elements; σ_2 on elements, wrinkled elements shown in grey.

Converged results obtained considering these four different methods were all in good agreement, as can be seen in Table 1, which compares some selected results obtained with SATS and Ansys models. In the Ansys model, the wrinkled elements detected in SATS presented very low but still positive 2nd principal stresses, possibly due to the post-processing extrapolations adopted by that program. Figure 3 compares displacement's norms and principal stresses on elements, obtained using SATS (differences of results through different methods are visually imperceptible, so figures are not repeated) and Ansys. In the plotting generated by SATS, principal directions are shown with lines of length proportional to the

stress magnitude. The wrinkled elements coincide for any alternative solution, and are displayed in grey, on the σ_2 plotting.

As expected, the use of the secant stiffness matrix $\tilde{\mathbf{K}}$ requires more Newton iterations for convergence, but each iteration is about 30% faster than the number-crunching finite difference procedure used to numerically calculate the tangent stiffness $\breve{\mathbf{K}}$. We also remark that, being a research program, SATS is implemented in MATLAB interpreted environment, and a lot of redundant calculations is performed, for the sake of readability, so the program is by no means optimized for speed, being much slower than Ansys, a compiled program.

8 AN INSUFFLATE DOME REINFORCED BY CABLES

Although results presented in the previous benchmark suggest that good results for problems of membrane wrinkling may be obtained using either the secant stiffness matrices $\tilde{\mathbf{k}}^e$ or the tangent stiffness matrices $\breve{\mathbf{k}}^e$, in fact only a few elements of the considered membrane did presented a wrinkled status. Besides, models with a small number of DOFs can be deceiving, in non-linear analysis.

In order to assess the performance of the alternative methods proposed above, in a large model, where wrinkling is more widespread, we consider as second application the large cable-reinforced, pneumatic envelope shown in Figure 4. It was designed to cover the site of a new nuclear power plant, during the process of ground preparation, remaining on site for only 6 months. The structure had a roughly rectangular plant, 110m x 86m, 30 meters high, and was anchored to a perimeter concrete wall. The membrane was reinforced by seven cables laid over the membrane, transversally constrained by fabric straps, but otherwise capable of sliding. A relatively small internal pressure $p_0 = 100 N/m^2$ was specified, and due to the short lifetime, a reduced basic wind pressure $q = 245 N/m^2$ was estimated. Figure 4(b) shows the membrane equilibrium configuration under internal pressure, adopted as initial configuration for wind analyses. In the present paper, we restrict our interest to comparing the convergence rates obtained considering $\tilde{\mathbf{K}}$ or $\breve{\mathbf{K}}$, and only for the case of the envelope constrained by adherent cables, under a transversal wind load, for which the wind pressure coefficients are given in Figure 4(c). We direct the reader to reference[8] for a detailed description of this system, as well as an explanation on the influence of cable sliding on its behavior.

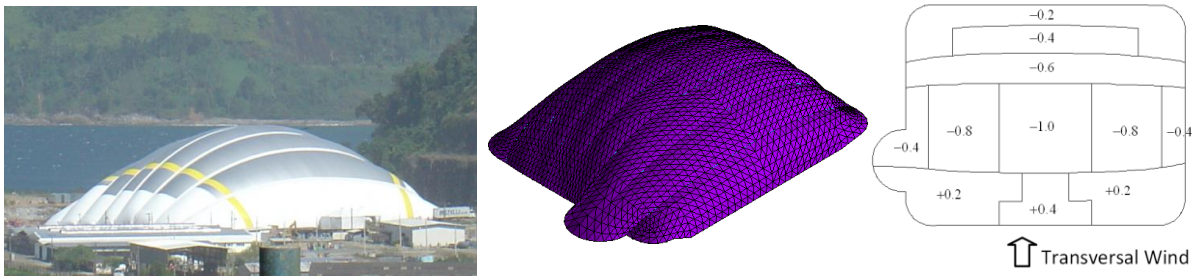

Figure 4 – (a) A large pneumatic dome reinforced by sliding cables; (b) equilibrium geometry under internal pressure; (c) wind pressure coefficients.

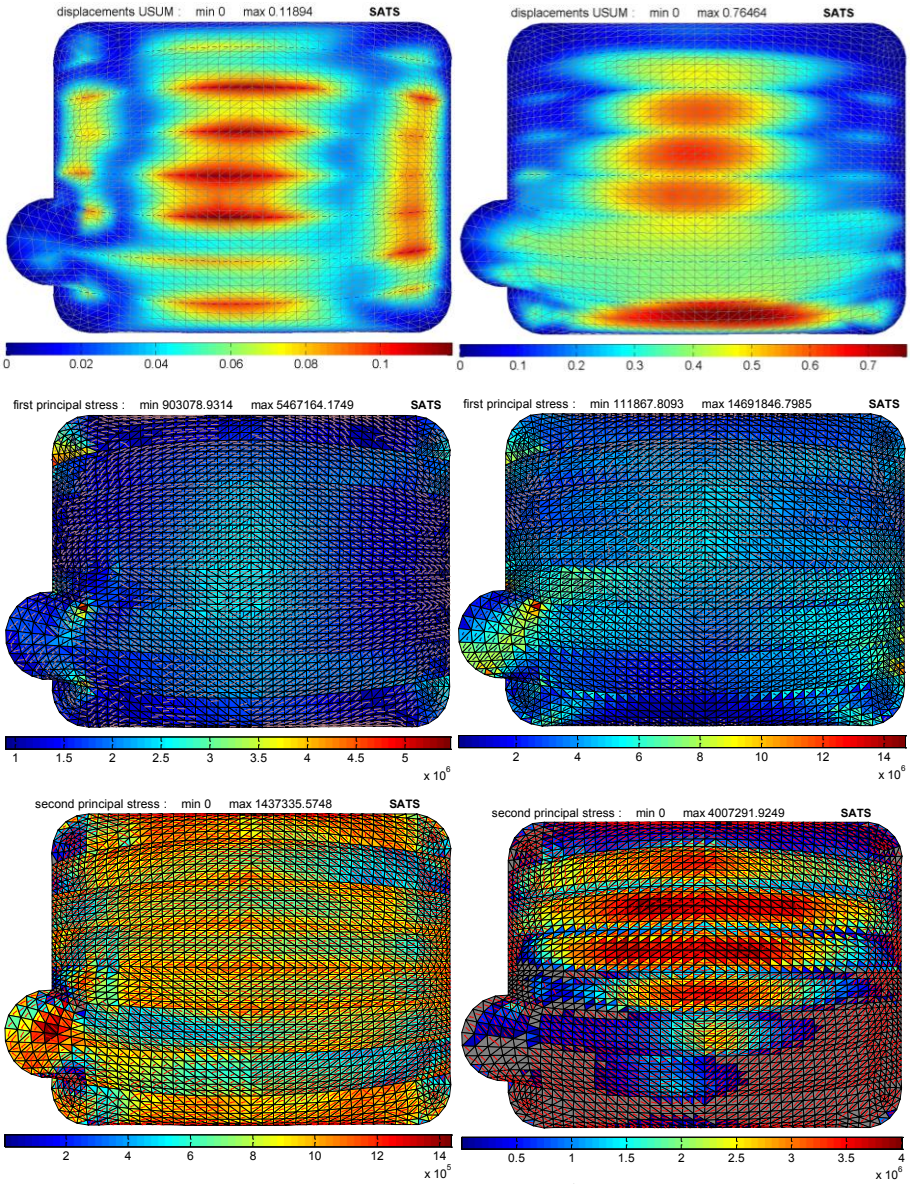

Figure 5: 1st column: results for internal pressure loads only; 2nd column: results for internal pressure plus transversal wind loads; 1st row: displacement norms; 2nd row: σ_1 on elements; 3rd row: σ_2 on elements, wrinkled elements shown in grey.

Table 2 shows some selected results for two load cases: "internal pressure" and "internal pressure + transversal wind", both with secant and tangent stiffness matrices. Figure 5 shows displacement norms, σ_1 and σ_2 stress fields for these two load cases. Differences between the alternative secant or tangent stiffness matrices are visually imperceptible, so results are not repeated. From top to bottom, Fig. 5 shows displacement norms, σ_1 and σ_2 stress fields. A large wrinkled zone is observed in the case of transversal wind loads (right column), at the wind side.

Table 2. Comparison of results for the pneumatic envelope, for two load cases $\left(\|\mathbf{g}\| / \|\mathbf{g}_0\|\right) \leq 10^{-4}$

Load case	"Internal pressure"		"Internal pressure + transversal wind"	
Stiffness matrix	Secant	Tangent	Secant	Tangent
Maximum displacement [m]	0.11894	0.11894	0.76464	0.76463
Maximum σ_1 [MPa]	5.46716	5.46718	14.69185	14.69122
Minimum σ_1 [MPa]	0.90308	0.90308	0.11187	0.11193
Maximum σ_2 [MPa]	1.43734	1.43733	4.00729	4.00730
Minimum σ_2 [MPa]	0.00000	0.00000	0.00000	0.00000
Number of iterations	9	6	25	8
Total time [s]	143.072	129.074	469,42	173.153
Time per iteration [s]	15.90	21.51	18.77	21.64

9 PROVISIONAL CONCLUSIONS

It was seen that both secant and tangent stiffness matrices are able to cope with the problem of membrane wrinkling, under the simplified assumptions describe above. When wrinkling is not widespread along the membrane, both secant and tangent matrices provide good convergence rates. On the other hand, when wrinkling is widespread, the secant stiffness renders convergence more difficult. Iteration cost also becomes larger for the secant stiffness, whilst it is practically invariant when the tangent stiffness is evaluated by finite differences. Therefore, although implementation of the secant matrix requires little extra computation when a linear-elastic material is already available, the finite difference approximation provides a systematic, straightforward way to keep quadratic convergence, requiring the sole definition of force vectors. At this point of research, this last is our preferable method.

REFERENCES

[1] R.M.O. Pauletti, D.M. Guirardi, T.E.C. Deifeld, 'Argyris' Natural Membrane Finite element Revisited', *STRUCTURAL MEMBRANES 2005,* Stuttgart, 2005.

[2] R.M.O. Pauletti, 'Static Analysis of Tension Structures', *Textile Composites and Inflatable Structures II*, Springer, 2008, E. Oñate, B. Kröpling (Eds.)

[3] T. Akita, K. Nakashino, M.C. Natori, K.C. Park, 'A simple computer implementation of membrane wrinkle behaviour via a projection technique', *Int. J. Numer. Meth. Engnr* **71**: 1231-1259 (2007).

[4] R.M.O. Pauletti, D.M. Guirardi, S. Gouveia, 'Modeling sliding cables and geodesic lines through dynamic relaxation', *IASS 2009 Symposium*, Valencia, 2009.

[5] R.M.O. Pauletti, E.S. Almeida Neto, 'A finite-difference approximation to Newton's Method Jacobian Matrices'. *IABSE-IASS Symposium*, London, 2011.

[6] R.M.O. Pauletti, E.S. Almeida Neto, 'A Finite-Difference Approximation to Newton Method's Jacobian matrices', *XXXI Iberian-Latin-American Congress on Computational Methods in Engineering, II South American congress on Computational Mechanics,* Buenos Aires, 2010.

[7] R.M.O. Pauletti, C.B. Martins, 'A Sliding-Cable Super-Element', *STRUCTURAL MEMBRANES 2009*, Stuttgart, 2009.

[8] R.M.O. Pauletti, 'Some issues on the design and analysis of pneumatic structures', *Int. J. Structural Engineering* **1**, (3/4): 217-240 (2010).